Мікроструктура сталі, поліпшеної мартенситним загартуванням та відпуском, змінюється з феріто-перлітної до мартенситної. Структура мартенситу має низьку зварюваність і низьку тріщиностійкість. Для поліпшення тріщиностійкості під час зварювання впоперек підводиться зовнішній магнітний потік (ВМП). Показано, що підвищення ВМП призводить до зниження швидкості поширення втомних тріщин

Ключові слова: швидкість поширення тріщин, тріщиностійкість, зовнішній магнітний потік, мартенситне загартування, мартенсит, сталь, поліпшена загартуванням та відпуском, зварюваність

Микроструктура стали, улучшенная мартенситной закалкой и отпуском, изменяется с феррито-перлитной до мартенситной. Структура мартенсита имеет низкую свариваемость и низкую трещиностойкость. Для улучшения трещиностойкости во время сварки поперечно подводится внешний магнитный поток (ВМП). Показано, что увеличение ВМП приводит к снижению скорости распространения усталостных трещин

Ключевые слова: скорость распространения трещин, трещиностойкость, внешний магнитный поток, мартенситная закалка, мартенсит, сталь, улучшенная закалкой и отпуском, свариваемость

UDC 338.45(075.8)
DOI: 10.15587/1729-4061.2018.122919

THE EFFECT OF EXTERNAL MAGNETIC FLUX FIELD IN THE QTS WELDMENT ON THE CHANGE OF FATIGUE CRACK PROPAGATION BEHAVIORS

Sugiarto
Associate Professor*
E-mail: sugik_mlg@ub.ac.id
Rudy Soenoko
Professor*
E-mail: rudysoen@yahoo.com
Anindito Purnowidodo
Associate Professor*
E-mail: anindito@ub.ac.id
Yudy Surya Irawan
Doctorate*
E-mail: yudysir@ub.ac.id
*Department of Mechanical Engineering
Brawijaya University Malang
Jalan. Mayjend Haryono, 167, Malang, Indonesia, 65145

1. Introduction

Hot roll quench tempered steel (QTS) is a heat-treated steel martempering of hot roll steel plate (HRSP) with a carbon content of 0.29 %. The process of hot rollers during the HRSP production process causes the grain structure to be tight and flat. With a heating process of 900 °C, held at that temperature for 10 minutes and the quenching process using water produces a small and tight metal grain structure and is dominated by a martensite structure. Furthermore, by providing a tempering process, by heating to a temperature of 300 °C, is held at that temperature of 10 minutes and cooled in air resulting in the final structure is tempered martensite. Martensite structures with small, denser granular structures possess less weldability so it is necessary to obtain certain treatments before, during or after welding [1–4].

2. Literature review and problem statement

With a microstructure dominated by a hard martensite structure, small but dense structures make QTS susceptible to cracking defects in both micro and macro scale. Microcracks are generally formed by combined voids or porosity [5]. Cracking of the micro in some time will trigger a crack that propagates or delay cracking. The welding cracks and delay cracking begins from the hydrogen diffusion or dissolved gases forming porosity, soluble inclusions and the difference in the rate of expansion and shrinkage of weld metal and HAZ during liquefaction and solidification of metals.

Crack propagation behavior is highly dependent on the variations of the failure parameters. Crack in metal is a defect in material structure due to the manufacturing process or formed during solidification [6]. Welds are generally the weaker parts in an assembly with an inherent risk of manufacturing defects which raises concerns regarding fatigue life and crack growth behavior in welded structural components [7]. The welding crack is generally divided into two categories: heat cracks which occur during the solidification process and cold cracks that occur during structural changes. The formation mechanism of hot cracking is related to metallurgical factors, stress, strain, and strain rate [8]. The heat crack occurs only in the weld area, whereas cold crack may occur in weld and HAZ areas [1]. Welding begins with the presence of diffusing hydrogen or dissolved gases, impurities deposits and the difference between expansion and shrink-

© Sugiarto, Rudy Soenoko, Anindito Purnowidodo, Yudy Surya Irawan, 2018

age of weld metal and parent metal during liquefaction and metal freezing. A welding defect in the form of a microcrack will trigger crack propagation [2].

Some previous studies investigated how welding parameters affected crack propagation on weld joints [7]. Traditional methods to improve the quality of weld joints mainly refer to the optimization of welding parameters [8]. Various welding parameters commonly used in the welding process are high current, long welding time, and high welding force to reduce crack propagation [9, 10]. External magnetic flux (EMF) field has been demonstrated to have a significant effect on the improvement of welding quality [7].

In metal welding using electric energy source, electromagnetic force (Lorenz forces), which affects the circulation of liquid metal in the weld pool will act. The rate of liquid metal circulation in the weld pool is also affected by the surface lift force (buoyancy force) and the force due to the surface tension (Marangoni force). Of the three forces acting on, the electromagnetic force gives the most dominant influence on the weld pool circulation [11]. Adding an external magnetic field during the spot welding resistance process (EMS-RSW) can improve the performance of DP780 welding and it increases the strength and plasticity of the weld [12].

Quenched and tempered steel is one of the primary manufacturing materials of steel pistons [13] and other applications. The application of EMF during welding may decrease the percentage of welding defects [14]. Welding of steel with martensite structure is very susceptible to cold cracking so it is advisable to do preheating and post-welding heating (PWHT) of martensitic steels. Preheating is done by heating at a temperature below Martensite start (Ms) before welding [3]. Welding thermal cycle has a negative effect on mechanical properties of martensitic stainless steel HAZ (P91) with Cr 8.81 % as the cause of cold cracking in HAZ. It is therefore advisable to provide preheating prior to welding of the material [4]. The EMF would affect the microstructures and microhardness of resistance spot welds. The HAZ of the welds under the external magnetic field would be softer than that of the traditional welds. Besides, the EMF could refine the columnar grain and increase the proportion of equiaxed grain in the nugget [7].

QTS has low weldability due to high defects in QTS welding area. High welded defects in QTS weld area are associated with microstructural changes of Hot Rolled Steel Plate (HRSP) during the hot rolling process, quenching process followed by tempering. The process of hot roll causes steel reduction by a tight and flat metal grain shape. Furthermore, the quenching process will form small and tight metal grains dominated by martensite structures.

Research on efforts to increase electromagnetic force and the effect of magnetic field on new welding process is done on base metal that has no microstructure changes. QTS is a general construction steel that has microstructure changes from ferrite + pearlite to martensite. Steel with martensite structures has a low weldability and is susceptible to crack propagation. In the previous study, the electromagnetic force was enhanced by raising the welding current. An increasing welding current will increase the weld heat input and thermal welding voltage. The high thermal stress results in large distortions and residual stresses after welding. The addition of EMF by raising the welding current on the QTS is susceptible to the rise of thermal stress and distortion and weld cracking. Increasing the electromagnetic force by adding EMF to the QTS is interesting to do. The EMF is generated by passing the DC current to the solenoid attached to the welding workpiece to avoid the rise of thermal tension.

In this research, a welding test to investigate crack propagation on Hot Rolled Quench Tempered Steel (QTS) with various EMF is performed. To improve QTS welding quality may be possible by increasing the liquid metal circulation rate prior to solidification. Because fast liquid metal circulation facilitates the release of gases and oxides to the surface of the weld pool. So, the quality of QTS welded results can be improved in the form of welding defects and welding cracks are lower and the weld toughness increases.

This research analyzes the quality of welded joints of QTS. QTS welding is very difficult because of its brittleness. This study discusses the phenomenon that occurs with the addition of EMF to increase the mechanical properties of QTS.

3. The aim and objectives of the study

The aim of the present research is to investigate the weldment QTS after addition of external magnetic flux.

To accomplish the set aim, the following tasks were set:

1. To assess the quality of QTS welded joints by addition of external magnet flux.

2. To increase delay cracking of QTS welded.

3. To investigate the behavior convection of molten metal effect on welding defects, inclusions, structural homogeneity and mechanical properties of welded joints.

4. To analyze the behavior of Hot Rolled Quench Tempered Steel (QTS) welding processes.

4. Materials and methods

4. 1. Convection on the weld pool

During welding using arc welding, the convection force will work on the weld pool resulting in the movement of liquid metal. The convection force is buoyancy force, marangoni force and electromagnetic force (F_L). The magnitude of the electromagnetic force is formulated: $F=J\times B$ [2], where J is the electric current density vector and B is the magnetic flux vector.

Electromagnetic force in the center of the weld pool will push the hot liquid metal down to the bottom of the pool, so the heat transfer that occurs leads to the bottom of the weld pool melt and weld pool deeper [1] as shown in Fig. 1.

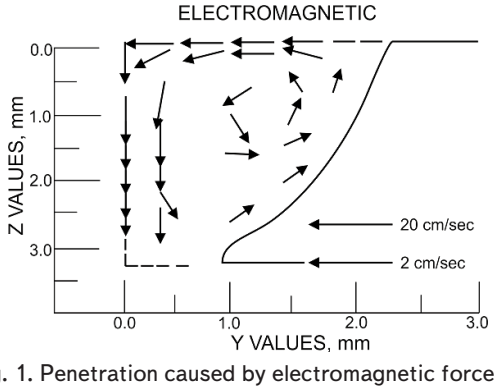

Fig. 1. Penetration caused by electromagnetic force [1]

The electromagnetic force with the resulting liquid metal circulation is instrumental in the process of mixing in the weld pool. This affects the homogeneity of structures in the weld pool. With the increase of electromagnetic force, the liquid metal circulation rate is getting bigger. The effect is that the effective value of thermal conductivity of liquid weld metal (*kL*) becomes larger so that the weld pool temperature becomes lower [15]. If the weld pool temperature drops, the post-welding cooling rate will also decrease and the weld toughness increases.

Increasing the electromagnetic force by increasing the welding current increases the heat input and creates residual stress, distortion, and changes in the microstructure [2].

4. 2. The rate of fatigue crack propagation

Cracks are assumed to develop through quasi-static incremental processes through crack propagation zones [16]. Internal pressure will decrease as cracks grow from the stress field [17]. According to Irwin, cracks can only propagate when the stress concentration factor (*K*) is the same as the critical stress concentration factor (K_{IC}) in the event of failure [18]. The crack growth will create two new surfaces and result in increased surface energy [19], and the new surface area produced at each fatigue cycle is proportional to the crack propagation rate [20]. In a ductile material, the plastic zone will develop at the tip of the crack. As the load increases, the plastic zone will increase in area until the crack grows and the material behind the tip of the crack opens. The plastic zone opening cycle near the crack tip causes the dissipation of heat energy [16]. So, crack propagation is an energy conversion process where the stress concentration factor or voltage intensity factor is a unique parameter that represents the magnitude of the stress field near the crack tip [6].

In the case of the loading of the crack, there are three models of crack openings occurring on the metal caused by three different loading patterns. Opening mode or mode I due to normal loading pattern to crack, sliding mode or II mode due to sliding loading pattern to crack and tearing mode or III mode due to loading pattern tearing crack [21].

The stress intensity factor (ΔK) in normal loading (mode *I*) for CT (Compact Tension) specimens, using the following equations,

$$\Delta K = \frac{\Delta P}{BW^{1/2}} \frac{(2+\alpha)}{(1-\alpha)^{3/2}} \times \times \left(0.886 + 4.64\alpha - 13.32\alpha^2 + 14.72\alpha^3 - 5.6\alpha^4\right), \quad (1)$$

with *K* – voltage intensity factor (MPa.m$^{1/2}$); *P* – outer force (tensile force) (Pa); *B* – plate thickness (mm); *W* – plate width (mm); $\alpha = a/W$ where $a/W \geq 0.2$.

The applications of the LEFM concept describe the growth behavior of cracks in area II. Crack propagation in this area can be explained by the Parisian equation. According to Paris, the crack growth will be generated when the applied load varies, even though the maximum voltage is lower than the critical duty. Paris formulates that the crack growth of each load cycle is a function of the stress intensity factor (ΔK), by the formula [21]:

$$\frac{da}{dN} = C(\Delta K)^n \text{ (mm/cycle)}, \quad (2)$$

with *n* – exponential coefficient; *C* – material constant; *a* – crack length (mm); *N* – number of loading cycles (cycle); ΔK – fluctuation of stress intensity factor (MPa·m$^{1/2}$); d*a*/d*N* – rate of fatigue crack propagation (mm/cycle).

In this case, **C** and **n** are experimentally determined constants. The smaller **n** price indicates the lower crack propagation rate and the greater **C** price indicates the material resistance to the increasingly larger cracks. ΔK is the difference between the maximum stress factor (Kmax) and the minimum stress factor (Kmin) written,

$$\Delta K = K_{maks} - K_{\min} \text{ (MPa·m}^{1/2}\text{)}. \quad (3)$$

The loading pattern used is sinusoidal with a constant amplitude cyclic load of Pmax and Pmin. Then the existing voltage is σmax and σmin and the voltage area is,

$$\Delta\sigma = \sigma_{\max} - \sigma_{\min}, \quad (4)$$

with the comparison of this voltage with a test only required variable voltage or maximum load. The ratio or voltage ratio (R) can be calculated by the equation

$$R = \frac{K_{\min}}{K_{maks}} = \frac{\sigma_{\min}}{\sigma_{maks}} = \frac{P_{\min}}{P_{maks}}. \quad (5)$$

4. 3. Experimental study

This study is an experimental study to analyze the effect of external magnetic flux (EFM) on the fatigue crack propagation rate of QTS welding area. External magnetic fluxes were added by passing DC electrical currents of 0, 3, 6, 9 and 15 Ampere through the solenoid transversally from two sides during the welding process. The number of coils of solenoid wire was 150. The DC currents flowed into the solenoid produce magnetic flux at the welding center of 0; 0.9; 1.7; 2.3 and 3.1 mT. The type of welding used was GMAW brand ESAB type Origo TM Mig C340 PRO with a CO2 protector. Welding current of 140 the existence of voltage 20 V for the type of flat position welding 1 layer. Electrode wire used was ER 70S-6 diameter 1 mm. Average welding speed of 15 cm/min and CO_2 flow rate of 12 liters/min. The thickness of the tensile test specimen and the fatigue crack propagation test was 5 mm.

Furthermore, the first tensile test was done to obtain the ultimate tensile strength of weld material. Tensile specimens were made according to AWS 4.0 standards. The ultimate tensile strength data was used to determine the maximum load on the fatigue crack propagation test. Testing of fatigue crack propagation rate using servo-hydraulic fatigue test was conducted. The fatigue crack propagation rate test was made based on ASTM E 647 standard. The crack initiation (a_0) was made 2 mm. The maximum load (Pmax) was taken 0.3 from the ultimate stress multiplied by the cross-sectional area of the test specimen. While the minimum load (Pmin) was taken 0. Fatigue load frequency 11 Hz. Test microstructure used Scanning Electron Microscope (SEM) with Nital etching solution. The percentage of welded defects was calculated from the microstructures photograph of the specimen on the weld area using the Image J software.

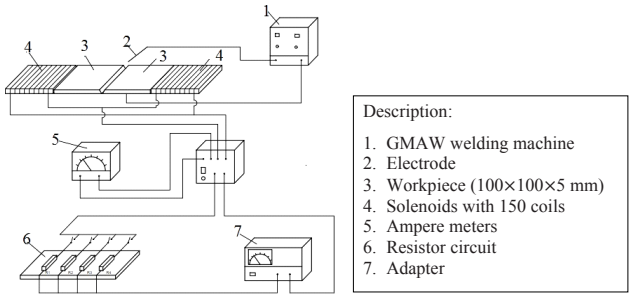

Fig. 2. Research Installation

Table 1

Elements contained in *QTS*

QTS	C, %	Si, %	Mn, %	S, %	Cr, %	Al, %	Cu, %	Mo, %
	0.29342	0.32985	1.41218	0.0081	0.55029	0.03785	0.08337	0.19303
	Ni %	P %	Pb %	Sn %	Ti %	V %	W %	Zn %
	0.27877	0.01425	0.00825	0.00339	0.00439	0.01473	0.00951	0.00378

5. Results

Tensile test results from each specimen due to the addition of magnetic flux and without the addition of magnetic flux (0 mT) can be seen in Table 2.

Table 2

Tensile Test Result Data

Magnetic Flux (mT)	*Ultimate Tensile Strength* (N/mm^2)
0	653.385
0.9	532.484
1.7	357.554
2.3	490.522
3.1	260.046

The ultimate tensile strength value from the tensile test results was used to determine the amount of load to be applied to the fatigue crack propagation test of each specimen. Testing the crack propagation rate was done by observing the number of load cycles and the change of crack length. Changes in crack lengths were observed using a digital microscope.

5. 1. The influence of EMF addition on the number of fatigue load cycles

The difference in a number of load cycles at the beginning of the crack opening shows the difference in the elasticity of the specimen until the beginning of the crack opening (Δa_1). In this case, Δa_1 is taken 10 % of the initial crack length of the test specimen (a_0) which is about 0.1×2 mm=0.02 mm. Specimens with a high number of load cycles at the beginning of the crack opening indicate a high degree of stiffness or elasticity.

From Fig. 3, it appears that the EMF addition of 0.7 mT and 1.7 mT causes the number of cycles to be lower than the specimen without the EMF addition (0 mT). This shows that the EMF addition of 0.9 mT and 1.7 mT during welding causes the QTS specimen to decrease the elasticity characteristic shown in the low number of cycles at the beginning of the crack opening. Furthermore, the EMF addition of 2.3 mT and 3.1 mT resulted in the higher number of cycles at the beginning of the crack opening than the specimen without the EMF addition. This indicates that the EMF addition of 2.3 mT and 3.1 mT leads to QTS elasticity at the beginning of the increased crack opening indicated by the difficulty of the initial crack formation.

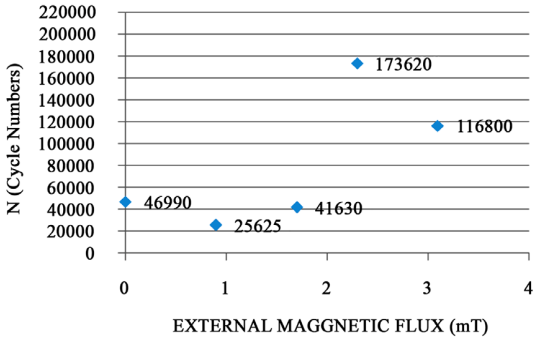

Fig. 3. The number of load cycles (*N*) at the start of the crack opening

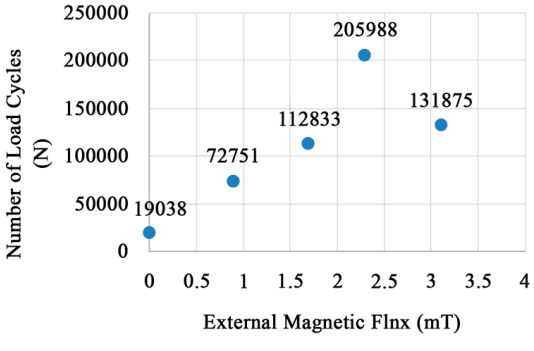

Fig. 4. The chart of the total number of load cycles (N) change due to the addition of magnetic flux (mT)

Fig. 4 shows that the EMF addition during welding causes the total number of fatigue load cycles to increase, which means the EMF addition causes the QTS specimen to be more resistant to crack propagation. The number of fatigue load cycles is increased by adding external magnetic flux from 0.9 to 2.3 mT, then it decreases again in the EMF addition of 3.1 mT.

5. 2. Main relation of EMF, length of cracks and number of fatigue load cycles

Fig. 5 shows that the EMF addition causes the fatigue crack propagation rate to be lower than the specimen without the EMF addition (0 mT). At the same crack length, the EMF addition of 0.9 to 2.3 mT causes the number of fatigue load cycles to increase and decrease again in the EMF addition of 3.1 mT.

The EMF addition of 3.1 mT resulted in liquid metal circulation in the weld pool too quickly. The fast convection rate causes inclusions of slag and rising oxides to be pulled back into the weld pool and trapped inside during the solidification process. In addition, the EMF addition that is too large during welding causes the welder difficult to control the rate of electrodes during the welding process.

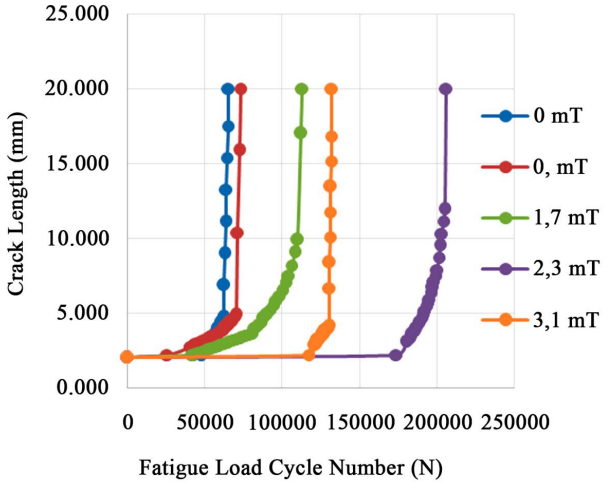

Fig. 5. The chart of the number of fatigue load cycles (*N*) changes to the crack length (mm) due to the addition of magnetic flux (mT)

5. 3. The relation of fatigue crack propagation rate (da/dN) to stress intensity factor (ΔK)

In Fig. 6, it appears that the EMF addition of 1.7 mT and 2.3 mT produces a graph that tends to slope. This indicates that the crack propagation rate of the QTS specimen is lower and resistance to the crack propagation is higher. Conversely, graphs that tend to upright show high crack propagation rate with low crack resistance.

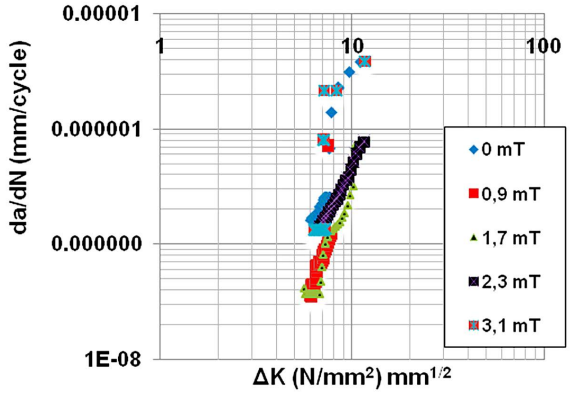

Fig. 6. The Chart of d*a*/d*N* vs Δ*K* due to magnetic flux addition (mT)

Fig. 7 shows the fatigue crack propagation graph (da/dN) vs. the stress intensity factor (Δ*K*) as described in equation 1. From Fig. 7 and Table 3, it appears that on QTS specimens with the addition of flux 0.9; 1.7; 2.3; and 3.1 mT showed a trend graph with a lower **n** value and a higher **C** value than the specimen without the addition of EMF (0 mT). This indicates that the addition of EMF results in slower fatigue propagation rates and toughness against crack propagation higher than QTS specimens without additional EMF.

The QTS specimen with the EMF addition of 2.3 mT results in the lowest crack propagation rate and the highest crack propagation resistance compared to other specimens indicated by the highest number of cycles, the smallest exponential graphic slope, the least **n** value and the biggest **C** value.

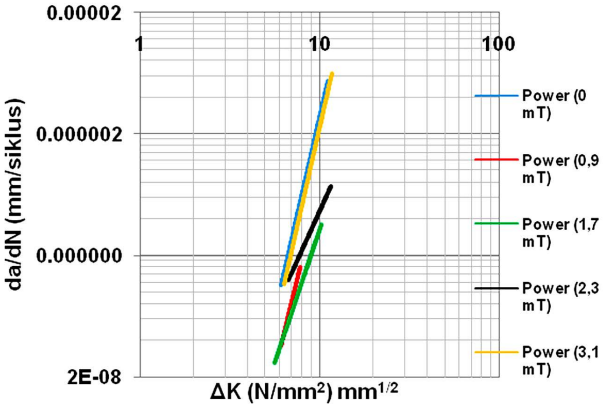

Fig. 7. Trendline of the relationship graph in da/dN vs ΔK

Table 3

The values of C and n of the trendline exponential (Fig. 7) of each specimen

Magnetic Flux (mT)	*C*	*n*	Equation
0	7E-13	6.5858	$Y0=7E-13\ X^{6.5858}$
0.9	5E-13	6.1498	$Y0,9=5E-13\ X^{6.1498}$
1.7	1E-11	4.3957	$Y1,7=1E-11\ X^{4.3957}$
2.3	3E-10	3.2692	$Y2,3=3E-10\ X^{3.2692}$
3.1	7E-13	6.5192	$Y3,1=7E-13\ X^{6.5192}$

5. 4. Analysis of structure of fracture section of fatigue crack propagation test result

Fig. 8 shows the effect of EMF addition on the structure of fracture section. Fig. 8, a presented the SEM image of fracture specimen 0 mT 2200× zoom. The presence of gaps or cavities that are still occurring and many inclusion defects in the weld metal specimen without the EMF addition is demonstrated.

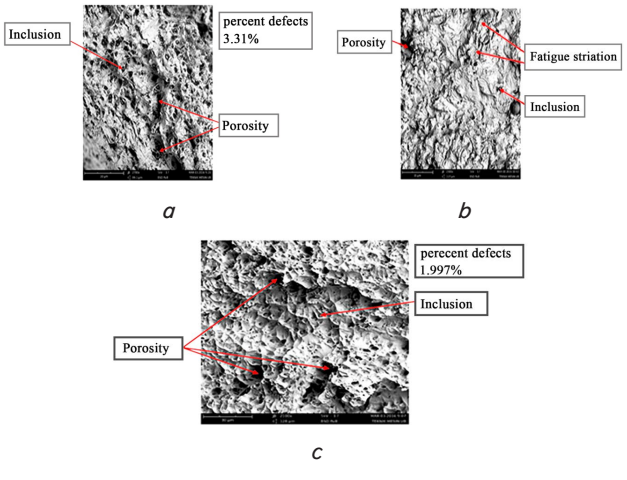

Fig. 8. SEM image of fracture specimen: *a* – 0 mT (without EMF); *b* – 2.3 mT; *c* – 3.1 Mt

The porosity and inclusion defects in this specimen are 3.311 % and more than in the specimen with the EMF addition. The largest percentage of defects is the number of load cycles possessed by the specimen without the EMF addition of 65246 cycles.

Fig. 8, *b* shows the SEM image of the microstructure of the specimen weld metal with the EMF addition of a 2.3 mT.

It appeared that the image still shows a little gap or cavity which is a porosity defect and inclusion defects with a percentage of 1,200 %. However, compared to other specimens, fewer defects occur. The number of cycles of load on the specimen with the EMF addition of 2.3 mT is the highest, which are 205,988 cycles. Fig. 8, *b* also shows fatigue striation that indicates the fault occurring is due to the fluctuating dynamic loads that occur over a long period of time and repeatedly experienced by the specimen.

Fig. 8, *c* shows the SEM photo of the specimen weld metal microstructure with the EMF addition of 3.1 mT. From the image, it appears there is still a gap or cavity which is a porosity defect and inclusion defects. Percentage of defects estimated 1.997 % formed at the time of crack formation is still lower than the specimen without the EMF addition. The crack opening is along the columnar crystal boundary, and fractures porosity defect, inclusion, as shown in the SEM images. The fatigue load cycle reached 131,875 cycles lower than the specimen with the EMF addition of 2.3 mT. Fig. 7 confirmed that the addition of EMF reduces defects in the weld metal.

6. Discussion of the effect of external magnetic flux field in the QTS weldment on the change of fatigue crack propagation behaviors

The EMF addition causes the electromagnetic forces acting on the weld pool to increase so that the liquid metal circulation rate also increases. The effect is that the mixing of the base metal and filler metal is more effective and the release of gas from liquid metal to the surface is also easier. The increasing number of fatigue load cycles indicates that the ductility of QTS specimens also increases. However, when the external magnetic flux is increased from 2.3 to 3.1 mT, the number of fatigue load cycles even decreases again. This is because the electromagnetic force which is too large causes the liquid metal circulation to be too fast compared to the speed of electrode feeding and it makes that the mixing of liquid metal between the base metal with filler metal becomes less effective.

Adding the EMF during welding will increase the electromagnetic force which impacts on increasing the circulation rate of liquid metal in the weld pool. As the rate increases, convection of liquid metal causes gas and inclusions can be lifted to the surface of the weld before solidification to reduce porosity defects and inclusions on welding metals. The lower welding defects and the more homogeneous welded structure make the specimen more resilient to crack propagation as indicated by the increasing number of fatigue load cycles and slower fatigue crack growth.

Adding a magneto-fluid dynamics mechanism to welding can alter the liquid metal stream conditions and increase the rate of liquid metal circulation in the weld pool [22]. The magnetic field strength affects the effect of protective gas, causing the penetration depth of the weld pool to increase by 7 % while the weld pool width of the change is not significant [23]. Adding an external magnetic field during the spot welding resistance process (EMS-RSW) can improve the performance of steel welding so that it increases the strength of the weld and plasticity [12].

Several studies related to the effect of magnetic field on the quality of welding results, among others, are done by Kern, et. al. 2,000 [22], which states that adding a magneto-fluid dynamics mechanism to laser beam welding can change the liquid metal lithium condition and increase the rate of liquid metal circulation in the weld pool. The use of low magnetic intensity during GMA welding on stainless steel 304 can increase HAZ corrosion resistance, increase the redistribution of Cr into austenite during thermal cycling, decrease sedimentation and growth of carbide chrome, Cr redistribution occurs continuously and films that increase HAZ corrosion resistance will be formed. In some of these studies, the electromagnetic force is magnified by increasing the welding current or welding current density (J) [22].

The effect of magnetic field on plasma control during CO_2 laser welding shows that magnetic field strength effect on protective gas effect, magnetic field strength causes weld pool penetration depth increase by 7 % while the width of weld pool is-not significantly changed [23].

Adding an external magnetic field during the spot welding resistance process (EMS-RSW) can improve the welding performance of DP780 thus increasing the weld strength and plasticity [25].

The electromagnetic force in the center of the weld pool will push the hot welding metal down to the bottom of the pool, so the heat transfer which occurs will result in the bottom of the weld pool melt and the weld pool deeper. The electromagnetic force with liquid metal circulation produced is very instrumental in the process of mixing (mixing) in the weld pool. This has an effect on the homogeneity of the composition in the weld pool [1].

When the magnet is placed in the longitudinal position against the welding, the magnetic force forces the electrons and ions in the arc causing the arc to be deflected from the normal arc path. As a result, there is a deflection in the welding arc that can change the nature of the weld bead. The penetration of the weld pool decreases and the width of the weld bead increases so that it affects the process parameters. Welded hardness decreases in the longitudinal direction and increases in the transverse direction. The EMF added longitudinally during welding affects the movement of electrons and ions in the welding arc, which causes the welding arc to be deflected from the direction of the normal arc. Welding arcs can be deflected forward, backward, or sideways depending on the direction of electrode displacement and weld direction due to the EMF effect. The impact of welding defects is reduced, hardness and tensile strength of weld metal increased due to grain structure improvement, weld toughness increased. While the EMF directed transverse causes hardness, tensile strength and toughness of the weld metal to decrease. An increase in EMF causes welding tensile strength to increase [25].

Electromagnetic stirring in the weld pool can significantly reduce the porosity of the weld bead, promote the growth of columnar grains and is able to withstand the tense cracks caused by sulfide [26]. Enlarging the electromagnetic force by increasing the welding current will increase the weld heat input, which is certainly not the right solution as it will raise the peak temperature of the weld and the cooling rate which can produce large thermal stresses. Enlarging the electromagnetic force by adding magnetic flux from the outset may be an alternative to increasing the circulation rate of liquid metal and lowering the weld peak temperature without being followed by an increase in thermal stress. Increasing rate of liquid metal circulation is supposed to able to repair the welding microstructure and HAZ, minimize

welding defects, minimize weld crack and increase fracture toughness.

Adding EMF during welding improves electromagnetic forces which impact on increasing the circulating rate of liquid metal in weld pools. The increasing rate of convection of liquid metal in the weld pool causes the gases and inclusions to lift the surface of the weld before solidification so as to reduce porosity defects and inclusions in welding metals. Lower welding defects and wider homogeneous welding structures cause the specimen to be more resilient to crack propagation as indicated by increasing number of fatigue loading cycles and slow crack growth, which means lower crack propagation rates.

With the addition of EMF of 3.1 mT, the convection rate at the weld pool is too fast. The fast convection rate allows inclusions of slag and rising oxides to be pulled back into the weld pool and trapped inside during the solidification process. Moreover, the addition of a magnetic flux which is too long after the welder has difficulty in controlling the electrode rate during the welding process. This is also confirmed by the description of the microstructural picture and the macro photo of the fracture surface in Fig. 8, *a–c*.

6. Conclusions

1. The effect of EMF is more sensitive to decrease the tensile strength and the fatigue crack propagation rate of the weld area. The result shows that the electromagnetic force on the weld pool increases. It causes the liquid metal circulation rate to increase and welding defects to decreases. This indicates that the liquid metal and filler metal are easily mixed, the release of gas from liquid metal to surface before solidification easily happens. The finding shows that the effect of EMF is more efficient. Percentage of defects of addition 3.1 mT estimated 1.997 % formed at the time of crack formation is still lower than the specimen without the EMF addition. The crack opening is along the columnar crystal boundary, and fractures porosity defect, inclusion. The fatigue load cycle reached 131,875 cycles lower than the specimen with the EMF addition of 2.3 mT.

2. QTS specimens with the EMF addition of 2.3 mT produces the smallest exponential slope graph, the smallest **n** value, and the greatest C value. This indicated low crack propagation and high toughness. The number of cycles of load on the specimen with the EMF addition of 2.3 mT is the highest, which is 205,988 cycles.

Acknowledgments

The authors are grateful to PT. Krakatau Steel and Ministry of Research, Technology, and Higher Education of the Republic of Indonesia. Sugiarto designed experiments majorly, performed the experiments, analyzed the data and wrote the paper, Soenoko R., Purnowidodo A. and Irawan Y. A. gave suggestions for improving this research.

References

1. Kou S. Welding Metalurgy. Wiley-interscience, New Jersey, 2002.
2. Messler R. W. Principles of Welding. John Wiley & Sons, 2004. doi: 10.1002/9783527617487
3. Béres L., Balogh A., Irmer W. Welding of Martensitic Creep-Resistant Steels // Welding Research. 2001. P. 191-s–195-s.
4. Microstructural Investigation of the Heat-Affected Zone of Simulated Welded Joint of P91 Steel / Vuherer T., Dunđer M., Milović L., Zrilić M., Samardžić I. // Metalurgija. 2013. Vol. 52, Issue 3. P. 317–320.
5. Khan Md. I. Welding Science and Technology. New Delhi: New Age International (P) Ltd., 2007. 278 p.
6. Chatterjee S., Doley B. Crack Propagation and Fracture Analysis In Engineering Structure By Generative Part Structural Analysis // International Journal Of Current Research. 2014. Vol. 6, Issue 06. P. 7032–7037.
7. Influence of dwell time on fatigue crack propagation in Alloy 718 laser welds / Iyer A. H. S., Stiller K., Leijon G., Andersson-Östling H. C. M., Hörnqvist Colliander M. // Materials Science and Engineering: A. 2017. Vol. 704. P. 440–447. doi: 10.1016/j.msea.2017.08.049
8. Experimental study of hot cracking at circular welding joints of 42CrMo steel / Zhang Y., Chen G., Chen B., Wang J., Zhou C. // Optics & Laser Technology. 2017. Vol. 97. P. 327–334. doi: 10.1016/j.optlastec.2017.07.018
9. Marya M., Gayden X. Development of Requirements For Resistance Spot Welding Dual-Phase (DP600) Steels Part 1: The Causes Of Interfacial Fracture // Welding Research. 2005. P. 172s–182s.
10. Joaquin A., Adrian N. A. E., Jiang C. Reducing shrinkage voids in resistance spot welds // Welding Research. 2007. P. 24–27.
11. De Herreran N. Computer Calculation of Fusion Zone Geometry Considering Fluid Flow and heat Transfer During Fusion Welding // Welding J. The Univ. of Texas at El Paso. 2003.
12. Impact of External Magnetic Field on Weld Quality of Resistance Spot Welding / Shen Q., Li Y., Lin Z., Chen G. // Journal of Manufacturing Science and Engineering. 2011. Vol. 133, Issue 5. P. 051001. doi: 10.1115/1.4004794
13. Li P. The Present Situation And Development Trend Of The Automobile Engine Piston Design. Autom. Tech. Mat. 2008. Vol. 1. P. 5–8.
14. The Use of Magnetic Flux to The Welding of Hot Roll Quench Tempered Steel / Sugiarto, Purnowidodo A., Sonief A., Soenoko R., Irawan Y. S. // ARPN Journal of Engineering and Applied Sciences. 2016. Vol. 11. P. 1061–1064.
15. Kostov I., Andonov A. Modelling of Magnetic Fields Generated by Cone Shape Coils for Welding with Electromagnetic Mixing // Journal of the University of Chemical Technology and Metallurgy. 2005. Vol. 40, Issue 3. P. 261–264.
16. Wang Z., Nakamura T. Simulations of crack propagation in elastic–plastic graded materials // Mechanics of Materials. 2004. Vol. 36, Issue 7. P. 601–622. doi: 10.1016/s0167-6636(03)00079-6
17. Sadananda K., Solanki K. N., Vasudevan A. K. Subcritical crack growth and crack tip driving forces in relation to material resistance // Corrosion Reviews. 2017. Vol. 35, Issue 4-5. doi: 10.1515/corrrev-2017-0034
18. Gürses E., Miehe C. A computational framework of three-dimensional configurational-force-driven brittle crack propagation // Computer Methods in Applied Mechanics and Engineering. 2009. Vol. 198, Issue 15-16. P. 1413–1428. doi: 10.1016/j.cma.2008.12.028

19. Hybrid discrete dislocation models for fatigue crack growth / Curtin W. A., Deshpande V. S., Needleman A., Van der Giessen E., Wallin M. // International Journal of Fatigue. 2010. Vol. 32, Issue 9. P. 1511–1520. doi: 10.1016/j.ijfatigue.2009.10.015
20. Effect of load amplitude change on the fatigue life of cracked Al plate repaired with composite patch / Albedah A., Khan S. M. A., Benyahia F., Bachir Bouiadjra B. // International Journal of Fatigue. 2016. Vol. 88. P. 1–9. doi: 10.1016/j.ijfatigue.2016.03.002
21. Broek D. Elementary Engineering Fracture Mechanic. 4th ed. Springer, 1982. 540 p.
22. Kern M., Berger P., Hügel H. Magneto-Fluid Dynamics Control Of Seam Quality In CO2 Laser Beam Welding // Welding Research Supplement. 2000. P. 72s–78s.
23. Tse H. C., Man H. C., Yue T. M. Effect of electric and magnetic fields on plasma control during CO2 laser welding // Optics and Lasers in Engineering. 1999. Vol. 32, Issue 1. P. 55–63. doi: 10.1016/s0143-8166(99)00045-7
24. Dar Y. A., Singh C., Farooq Y. Effects of External Magnetic Field on Welding Arc of Shielded Metal Arc Welding // Indian Journal of Applied Research. 2011. Vol. 4, Issue 4. P. 200–203. doi: 10.15373/2249555x/apr2014/60
25. Senapati A., Mohanty S. brata. Effects of External Magnetic Field on Mechanical properties of a welded M.S metal through Metal Shield Arc Welding // International Journal of Engineering Trends and Technology. 2014. Vol. 10, Issue 6. P. 297–303. doi: 10.14445/22315381/ijett-v10p258
26. Metallurgical Characterization of API X65 Steel Joint Welded by MIG Welding Process with Axial Magnetic Field / Natividad C., García R., López V. H., Contreras A., Salazar M. // Materials Research. 2017. Vol. 20, Issue 5. P. 1174–1178. doi: 10.1590/1980-5373-mr-2016-0182

Досліджено вплив робочих параметрів плазмово-електролітичного оксидування у дифосфатному кобальтвмісному електроліті на процес формування оксидних покривів на сплаві АЛ25. Встановлено, що склад та морфологія поверхні одержаних шарів $Al_2O_3{\cdot}CoO_x$ залежать від густини струму обробки та часу оксидування. Варіювання параметрів ПЕО дозволяє гнучко керувати процесом інкорпорації каталітичного компоненту в матрицю оксиду основного металу. Обгрунтовано раціональний режим обробки поршневого силуміну для формування збагачених кобальтом оксидних покривів

Ключові слова: поршневий силумін, АЛ25, плазмово-електролітичне оксидування, оксидний покрив, морфологія поверхні

Исследовано влияние рабочих параметров плазменно-электролитического оксидирования в дифосфатном кобальтсодержащем электролите на процесс формирования оксидных покрытий на сплаве АЛ25. Установлено, что состав и морфология поверхности сформированных оксидных слоев $Al_2O_3{\cdot}CoO_x$ зависят от плотности тока обработки и времени оксидирования. Варьирование параметров ПЭО позволяет гибко управлять процессом инкорпорации каталитического компонента в матрицу оксида основного металла. Обоснован рациональный режим обработки поршневого силумина для получения обогащенных кобальтом оксидных покрытий

Ключевые слова: поршневой силумин, АЛ25, плазменно-электролитическое оксидирование, оксидное покрытие, морфология поверхности

UDC 621.35
DOI: 10.15587/1729-4061.2018.128457

STUDY OF THE INFLUENCE OF OXIDIZING PARAMETERS ON THE COMPOSITION AND MORPHOLOGY OF $Al_2O_3{\cdot}CoO_x$ COATINGS ON AL25 ALLOY

A. Karakurkchi
PhD, Senior Researcher*
E-mail: anyutikukr@gmail.com
M. Sakhnenko
Doctor of Technical Sciences,
Professor, Head of Department**
E-mail: sakhnenko@kpi.kharkov.ua
M. Ved'
Doctor of Technical Sciences, Professor*
E-mail: vmv@kpi.kharkov.ua
Department of Physical Chemistry*
*Department of General and Inorganic Chemistry***
***National Technical University
«Kharkiv Polytechnic Institute»
Kyrpychova str., 2, Kharkiv, Ukraine, 61002

1. Introduction

Alloying of silumins with additional components allows great expansion of the scope of their application. Al-Si alloys are successfully applied in various industries, specifically for manufacturing parts of a cylinder-piston group of internal combustion engines (ICE) [1, 2].

Additional techniques of surface modification are effectively used for improvement of mechanical properties of silumins. One of the approaches involves electrochemical

© A. Karakurkchi, M. Sakhnenko, M. Ved', 2018